Int J CARS
DOI 10.1007/s11548-015-1228-8

ORIGINAL ARTICLE

Model-based segmentation in orbital volume measurement with cone beam computed tomography and evaluation against current concepts

Maximilian E. H. Wagner[1] · Nils-Claudius Gellrich[1] · Karl-Ingo Friese[2] · Matthias Becker[3] · Franz-Erich Wolter[2] · Juergen T. Lichtenstein[1] · Marcus Stoetzer[1] · Majeed Rana[1] · Harald Essig[4]

Received: 5 December 2014 / Accepted: 20 May 2015

Abstract
Purpose Objective determination of the orbital volume is important in the diagnostic process and in evaluating the efficacy of medical and/or surgical treatment of orbital diseases. Tools designed to measure orbital volume with computed tomography (CT) often cannot be used with cone beam CT (CBCT) because of inferior tissue representation, although CBCT has the benefit of greater availability and lower patient radiation exposure. Therefore, a model-based segmentation technique is presented as a new method for measuring orbital volume and compared to alternative techniques.
Methods Both eyes from thirty subjects with no known orbital pathology who had undergone CBCT as a part of routine care were evaluated ($n = 60$ eyes). Orbital volume was measured with manual, atlas-based, and model-based segmentation methods. Volume measurements, volume determination time, and usability were compared between the three methods. Differences in means were tested for statistical significance using two-tailed Student's t tests.
Results Neither atlas-based ($26.63 \pm 3.15\,mm^3$) nor model-based ($26.87 \pm 2.99\,mm^3$) measurements were significantly different from manual volume measurements ($26.65 \pm 4.0\,mm^3$). However, the time required to determine orbital volume was significantly longer for manual measurements (10.24 ± 1.21 min) than for atlas-based (6.96 ± 2.62 min, $p < 0.001$) or model-based (5.73 ± 1.12 min, $p < 0.001$) measurements.
Conclusion All three orbital volume measurement methods examined can accurately measure orbital volume, although atlas-based and model-based methods seem to be more user-friendly and less time-consuming. The new model-based technique achieves fully automated segmentation results, whereas all atlas-based segmentations at least required manipulations to the anterior closing. Additionally, model-based segmentation can provide reliable orbital volume measurements when CT image quality is poor.

Keywords Orbital volume · Pseudoforamina · Model segmentation · Cone beam computed tomography

Introduction

The highly complex orbit contains the eye and its appendages. It is made up of seven bones and serves to protect the eye from mechanical injury [1]. The complex three-dimensional (3-D) anatomy of the orbit makes diagnosis and treatment of various orbital region diseases challenging. Therefore, highly accurate orbital assessments are crucial in managing orbital diseases [2], and reliable, high-quality control measurements are the cornerstone of properly diagnosing orbital diseases. Evaluators should remember to consider the influence of ocular swelling and compensations from recent orbital anatomy changes or iatrogenic interventions [3]. The fellow orbit can serve as a control for the affected orbit for pre- and postoperative evaluations because the unaffected eye will not have the soft tissue swelling that often occurs after surgery. There-

✉ Maximilian E. H. Wagner
m.e.h.wagner@icloud.com

1 Department of Craniomaxillofacial Surgery, Hannover Medical School, Carl-Neubergstrasse 1, 30625 Hannover, Germany

2 Institute for Man-Machine Communication, Leibniz University Hannover, Hannover, Germany

3 MIRALab, University of Geneva, Geneva, Switzerland

4 Department of Craniomaxillofacial Surgery, University Hospital Zürich, Zurich, Switzerland

Published online: 05 June 2015

fore, an objective method to obtain quality orbital volume measurements in patients is necessary.

Orbital volume measurements can be obtained by segmenting the bony frame of the orbital walls and by accurate determination of the anterior and posterior closing of the orbital cavity. Each segmentation application has to handle two major challenges in the orbital region stemming from the thin bony areas of the orbital floor and medial orbital wall. First, these regions are often misrepresented in the 3-D data set, mainly because of efforts to decrease radiation, and cannot be used with certain segmentation methods (e.g., threshold-based segmentation). These areas often appear as holes in the 3-D data set, even though the bone is intact. Therefore, these holes are often called pseudoforamina [4]. Second, imaging modalities like CBCT are becoming increasingly important because of their low cost, lower patient radiation exposure, and increased availability [5,6]. However, bone segmentation in the thin orbital regions can be challenging on CBCT scans because of differences from traditional CT scans due to beam hardening and inhomogeneity [7].

Various efforts have been made to create reliable orbital segmentation and measurement methods. The four methods currently available are manual, threshold-based, atlas-based, and model-based segmentation. Manual segmentation is solely defined by the user. Evaluators need to mark the borders of an object by hand in each image slice. This method is accurate, can be used in virtually all imaging modalities, and is therefore often used as a golden standard when evaluating the error of other segmentation techniques; however, it requires skill and experience [8–10]. Manual segmentation used to be routinely employed in computer-assisted surgery, but is now reserved for very complex or unique tasks. Threshold-based segmentation is based on the fact that each tissue is represented by a unique Hounsfield unit (HU). These values can be used to segment structures with the same radiological properties in a specific area. Unfortunately, this segmentation method cannot be reliably used for bony orbital frame segmentation, largely because of pseudoforamina [11]. Atlas-based segmentation bases volume measurements on characteristic landmarks of an intact skull. A template is created based on these landmarks, which is then used on the specified region of interest [12]. During the registration process, segmentation results are fit to exact area dimensions [13,14]. Localized discrepancies between the registration processes and desired segmentation results can be manually corrected retrospectively by local deformation tools. Therefore, this method can be used for orbital volume segmentation. Model-based segmentation involves estimating the expected shape of segmentation (e.g., intraorbital volume) and placing it in the desired segmentation area. By expanding and deforming the model-based shape to fit the underlying image data set, the desired segmentation can be acquired [15,16]. Model-based segmentation approaches can use different means of expressing prior knowledge such as labels or constraints on the initial shape. Labels are sets of key–value pairs. They can be attached to vertices, edges, or triangles and contain parameters for the deformation. Typical scenarios are stronger smoothing near foramina or the preservation of a sharp edge. Another approach comprises statistical shape models that express the principal components of variation based on a large sample number [17]. Deformable models are a subgroup of model-based segmentation approaches [18,19] that have been successfully applied to many scenarios, including the heart [20,21], femur [22], and liver [23]. Non-fully automated model-based segmentation approaches can be user-guided [24] or interact using haptic devices [25]. Orbit segmentation has proven to be a good application for deformable models [24,25], especially with the support of statistical shape models [17].

Manual, threshold-based, and atlas-based segmentation are currently used in clinical practice for diagnosing patients and for planning surgical procedures. However, only manual and atlas-based segmentation methods are used for proper orbital volume measurement. Model-based segmentation is rarely used, but may be a good option for overcoming the challenges of pseudoforamina and varying image characteristics between scanning modalities. Here, we compare manual, atlas-based, and model-based segmentation used to measure orbital volume. To the best of our knowledge, this is the first time model-based segmentation has been used to measure orbital volume and the first time the results are directly compared to other orbital volume measurements. Segmentation accuracy, ease of use, and time needed to determine orbital volume were specifically examined.

Methods

This study was approved by the institutional ethics committee (MHH 2477-2014), which waived the need for informed consent. All study procedures adhered to the tenets of the Declaration of Helsinki. Thirty patients with no known orbital region pathology were selected for study inclusion. All patients had undergone CBCT scanning (PaX-Zenith 3D, VaTech, Fort Lee, NJ) of the skull as part of their standard-of-care clinical course. Orbital volume is often used to objectively compare the characteristics of the affected and unaffected orbit in the same patient (e.g., following unilateral orbital reconstruction). Therefore, the volume of both orbits was measured in all 30 patients ($n = 60$ orbits) using manual segmentation, atlas-based segmentation, and model-based segmentation. Measurement accuracy, time expenditure, and

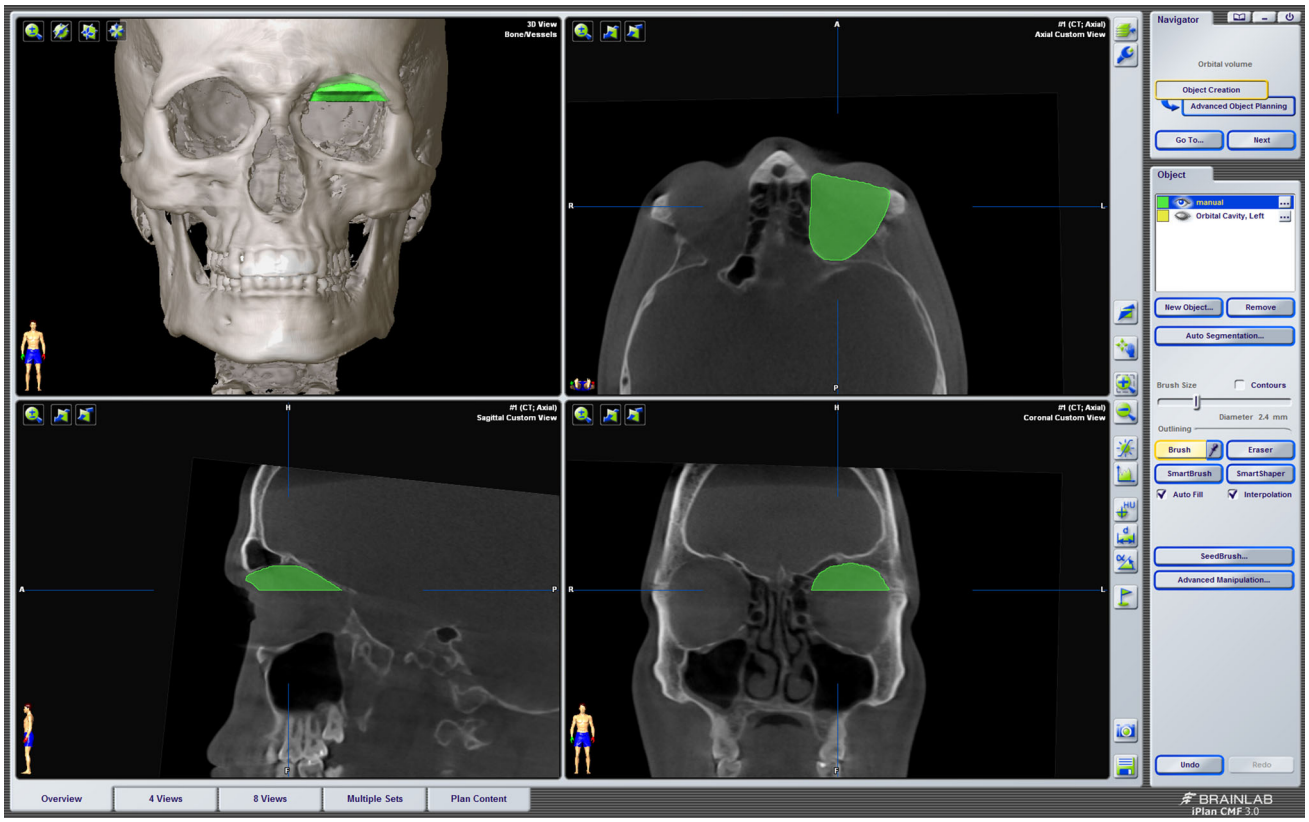

Fig. 1 Manual segmentation of each slice of the *left* orbit using iPlan 3.0.5 software. Segmented orbital volume can be controlled in real time in three dimensions or in axial, coronal, and sagittal views

ease of use were compared between the three measurement methods. All orbital volume segmentation was performed on a standard personal computer (Windows® 7, Intel® Core i7, 8GB RAM).

Manual segmentation was performed using the brush tool in the iPlan® 3.0.5 software (Brainlab, Feldkirchen, Germany). Orbital area had to be manually marked in every slice of the data set for each orbit. The software then interpolated the region between slices and calculated the 3-D volume of the orbit (Fig. 1). To exclude inter-observer variability arising from the dependency of the particular segmentation technique on the user's experience, three different surgeons with multiple years of clinical expertise performed manual segmentation independently on each orbit.

Atlas-based segmentation was also performed using the iPlan 3.0.5 software. For this method, the cavity tool, an atlas function for orbital volume segmentation, was used. The software's registration algorithm automatically adjusts the atlas template to fit the orbital shape of the CBCT data set. The volume of the object is then calculated and displayed (Fig. 2). If necessary, changes can be manually made to the 3-D object using the software's local deformation function smart shaper (e.g., to adjust the anterior closing or the border between segmented objects and adjacent bony structures, Fig. 3).

Model-based segmentation was performed using the YaDiV program with a special orbital volume segmentation tool [26,27]. After properly placing the orbital model at the region of interest, orbital volume was automatically calculated (Fig. 4), as described below. The shape of the orbital model we chose was based on a manual intraorbital segmentation of an intact orbit of the respective side, with a decrease to 2/3 of the original size. The size can be adjusted in the program, although this was not necessary in our cases. The model of the respective side was placed manually roughly inside the orbital borders. Exact placement, i.e., complete placement inside the desired area, did not affect the final segmentation result, as both growth and shrinkage are possible during model-based segmentation. Three basic forces (a growing force, a smoothing force, and an image force) are used to control model expansion and to create the proper orbital segmentation. The growing force is applied to the complete model for each vertex ($\boldsymbol{v}_i$) directed along the normal ($\boldsymbol{n}_i$) and adjusted by factor s_b in the following manner:

$$F^b(\boldsymbol{v}_i) = s_b \boldsymbol{n}_i$$

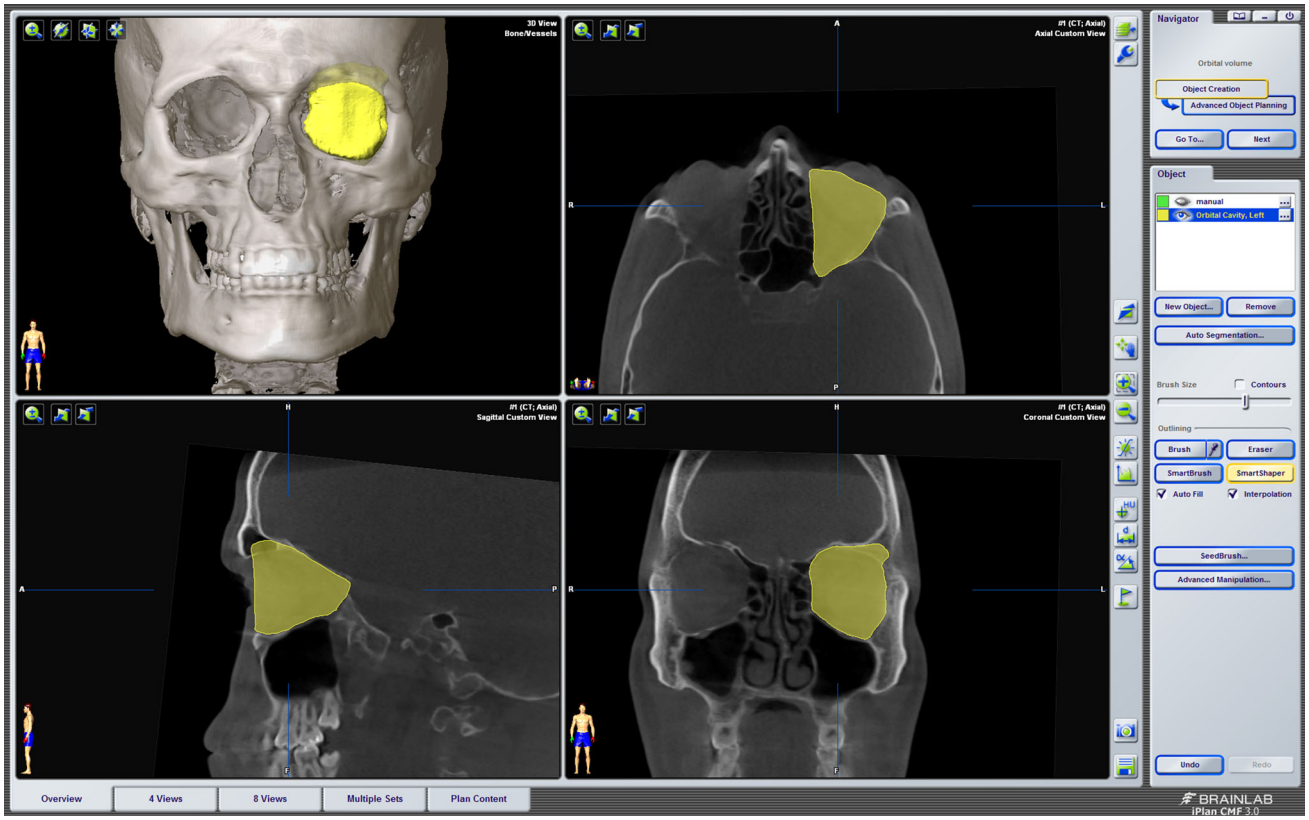

Fig. 2 Atlas-based segmentation of the *left* orbit using iPlan 3.0.5 software. Laterocranial segmentation correction was needed due to software segmentation error

A Laplacian smoothing force is then applied in the following manner to avoid model "leakage" through pseudoforamina or other geometric orbital openings. Single vertices are pulled more strongly toward neighbors that are farther away, and single vertices passing through pseudoforamina would be pulled back by the smoothing force:

$$F^s(\boldsymbol{v}_i) = \frac{s_s}{\left|U_{\boldsymbol{v}_i}(\Delta)\right|} \sum_{\boldsymbol{u} \in U_{\boldsymbol{v}_i}(\Delta)} (\boldsymbol{u} - \boldsymbol{v}_i),$$

where $U_{\boldsymbol{v}_i}(\Delta)$ are the neighboring vertices of $\boldsymbol{v}_i$ reachable through up to Δ edges, which determines the size of the neighborhood, vertex $\boldsymbol{u}$ is a member of $U_{\boldsymbol{v}_i}(\Delta)$, and s_s is an adjustable factor. The forces are normalized to compensate for different sizes of neighborhoods. The summed vector differences cancel each other out if they have different directions and similar distances to the center. However, if not, the result is a force in the direction of distant neighbor vertices that aims at preventing holes.

Finally, an image force is used to adapt the model to the actual image data. Because of inconsistent HU mapping in CBCT, the gradient has been used rather than the intensity profile. This was performed using the following equation:

$$F^i(t_j) = -s_i \boldsymbol{n}_j \sum_{\boldsymbol{x}_t \in t_j} \sum_{\delta=\delta_b}^{\delta_f} k(\delta) * g\left(\boldsymbol{x}_t + \delta \cdot \boldsymbol{n}_j\right),$$

where $F^i(t_j)$ is the image force for triangle t_j. For every voxel x_t cut by t_j, the normalized image gradient $g()$ has been calculated on δ_f layers in front of t_j and δ_b layers behind t_j. The gradients have been scaled using a layer-dependent scaling factor $k(\delta)$ and then summed. They scale the force along the normal $\boldsymbol{n}_j$ of t_j. The resulting force is adjusted using the factor s_i.

One challenge of using this model is the proper positioning of the anterior closing. After model expansion over the orbital border (no anterior external force to stop model expansion), the concave borders of the periorbital rim region define the closing path. This is the preferred method to independently determine the anterior closing surface for each orbit [28,29]. All segmented areas in front of that path are removed from the final orbital volume segmentation.

In addition to the volume and time for all three segmentation methods described above, the ease of use of each method was also evaluated. Therefore, three experienced users were

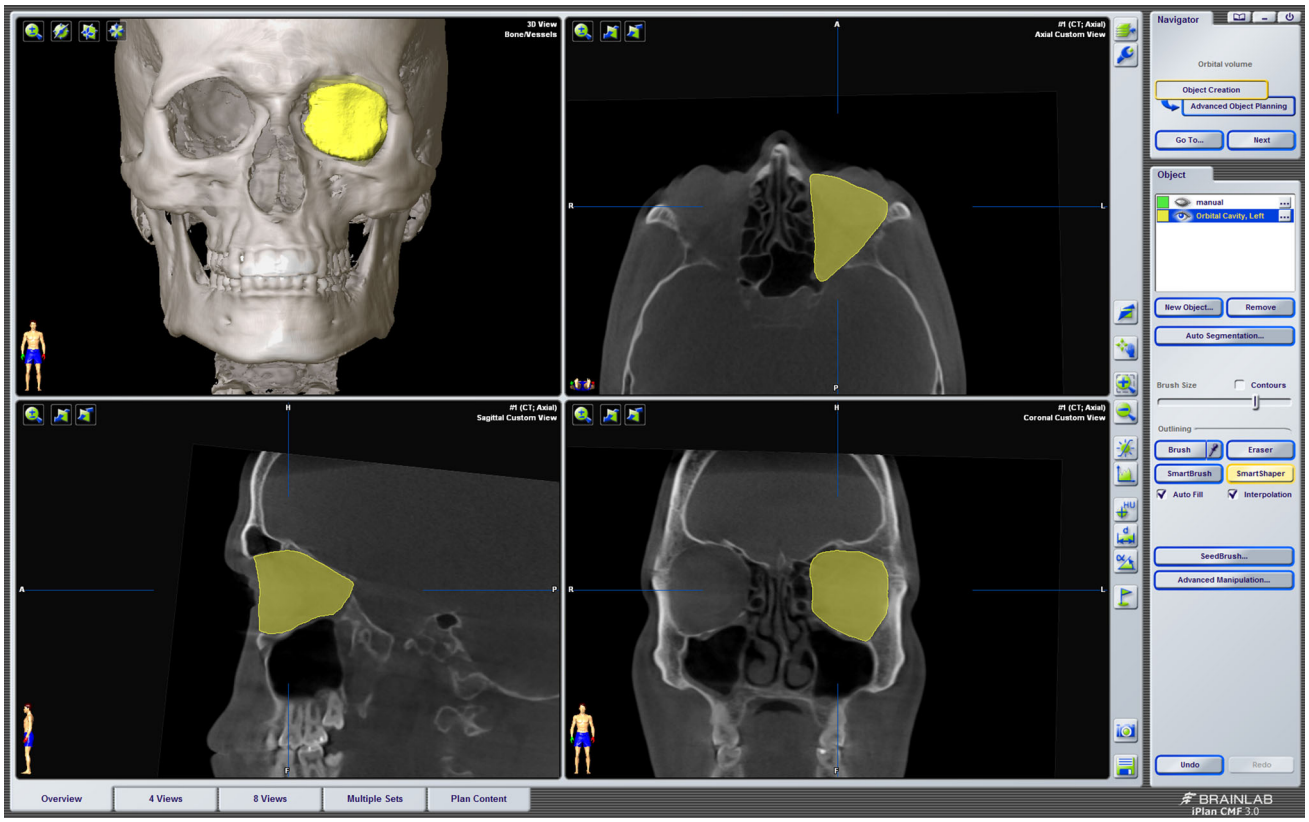

Fig. 3 Atlas-based segmentation of the *left* orbit using iPlan 3.0.5 software. Segmentation correction with a local deformation tool was needed to obtain these results

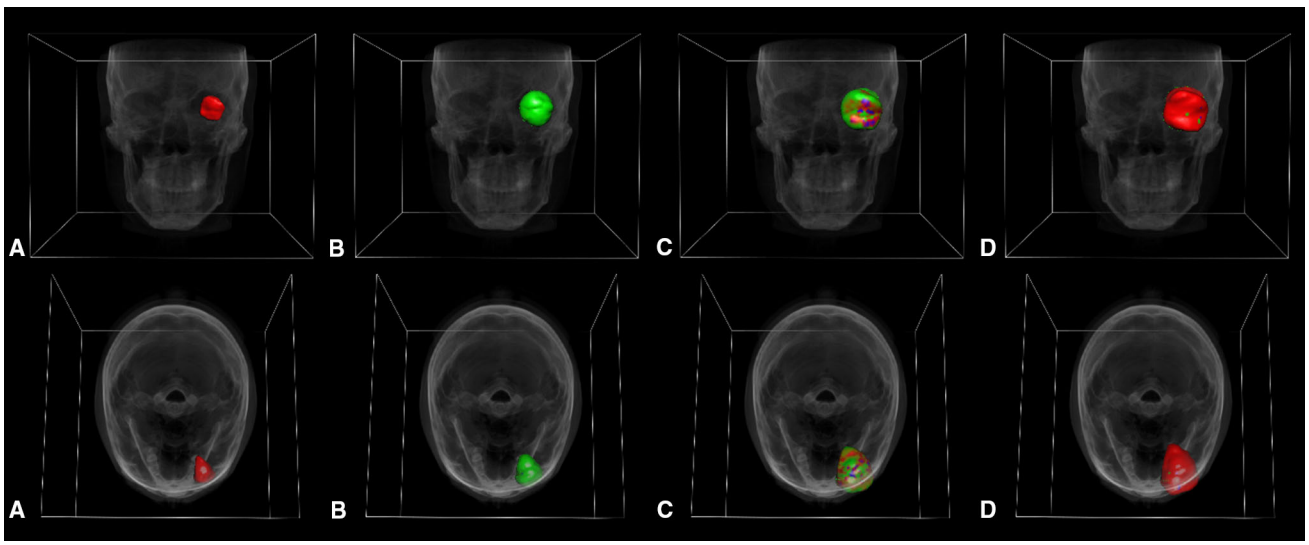

Fig. 4 **a** Model placement in the orbital region. **b** Growing the model (*green voxels*). **c** If growing forces at a voxel are in equilibrium after several expansion steps, expansion at that voxel is halted (*red voxels*). **d** Final model after global termination of expansion

asked to use a five-point scale to subjectively rate manual adjustment needs, usability, and the need for clinical experience.

All data analyses were performed using SigmaPlot® (version 12.0, Systat Software, Inc., San Jose, CA). Statistical significance of differences in means was examined using two-tailed Student's t tests. To exclude inter-observer variability in manual segmentation, a one-way ANOVA was performed. Statistical significance was defined as $p \leq 0.05$.

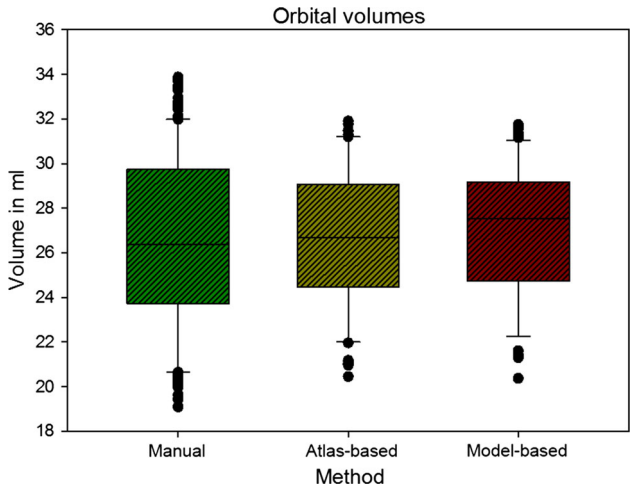

Fig. 5 *Boxplots* showing orbital volume results with manual, atlas-based, and model-based segmentation. Each data point represents one measurement. *Error bars* represent one standard deviation from the mean. Orbital volume was not significantly different between measurement methods

Results

In total, 12 female and 18 male patients were included in analyses. The mean orbital volume determined using manual measurement, the current gold standard, was $26.65 \pm 4.0\,\text{mm}^3$. There was no significant difference between the three experienced surgeons ($p = 0.476$). Atlas-based and model-based volume determinations resulted in a mean orbital volume of $26.63 \pm 3.15\,\text{mm}^3$ and $26.87 \pm 2.99\,\text{mm}^3$, respectively (Fig. 5). The manual orbital volume measurement was not significantly different from either the atlas-based ($p = 0.865$) or the model-based ($p = 0.785$) measurement. An example of each orbital segmentation method is shown in Fig. 6.

The time needed to determine orbital volume with each of the three methods was measured. Manual, atlas-based, and model-based orbital volume measurement took an average of 10.24 ± 1.21, 6.96 ± 2.62, and 5.73 ± 1.12 min, respectively (Fig. 7). This time includes loading the patient information in the software, measuring the volume with the respective tool, and adjusting the result to the bony borders of the orbit if necessary. The pure time required to segment the orbit manually and the pure run time for the atlas-based and model-based segmentation were 9.54 ± 0.94, 0.59 ± 0.1, and 0.84 ± 0.1 min, respectively. Although atlas-based segmentation was faster with regard to pure run time, because of the corrections required, model-based volume determination was significantly faster than both manual and atlas-based measurements in overall segmentation time ($p < 0.001$). The atlas-based method was also significantly faster than the manual method in overall segmentation time ($p < 0.001$). The atlas-based method was slower than the model-based method because of the extensive need to manually correct volume segmentation. On the one hand, the anterior closing had to be performed in each orbit; on the other hand, in almost half of all segmented orbits, mis-segmentation caused by a closed sinus or thin bony structures such as the medial orbital wall had to be corrected. In the model segmentation, correction was necessary for five orbits, exclusive to the medial orbital wall. Errors in segmentation are shown as spikes in the boxplot in Fig. 7.

The results of the usability assessment are shown in Table 1. The final volume segmentation required almost no adjustments when using manual segmentation, but had a low usability rating and a high need for clinical experience. The atlas-based segmentation required some adjustments as shown in Fig. 3. Most of these corrections were necessary in close vicinity to the frontal sinus or the thin medial orbital wall. The difference between the complete time necessary for calculation and the run time of the segmentation only reveals that the correction required a considerable amount of time in atlas-based segmentation. Usability was considerably higher, and the demand for clinical experience was lower (rated moderate). The model-based segmentation required some manual adjustments in rare cases. If necessary, the medial wall of the orbit was affected almost exclusively. Usability with model-based segmentation was rated as high, and the need for clinical experience was rated as low.

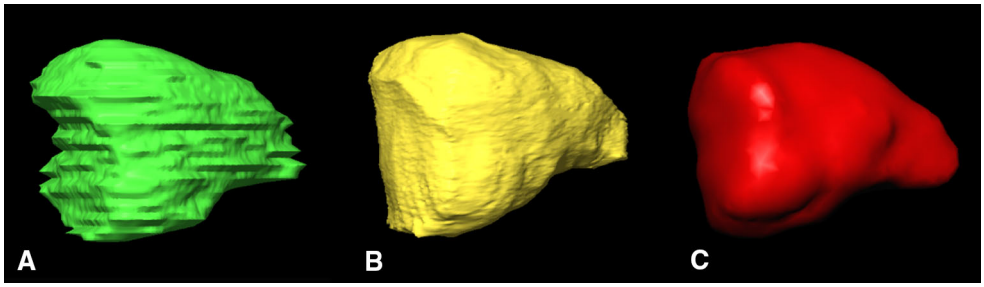

Fig. 6 Three-dimensional reconstruction of the same orbit using manual (**a**), atlas-based (**b**), and model-based (**c**) segmentation

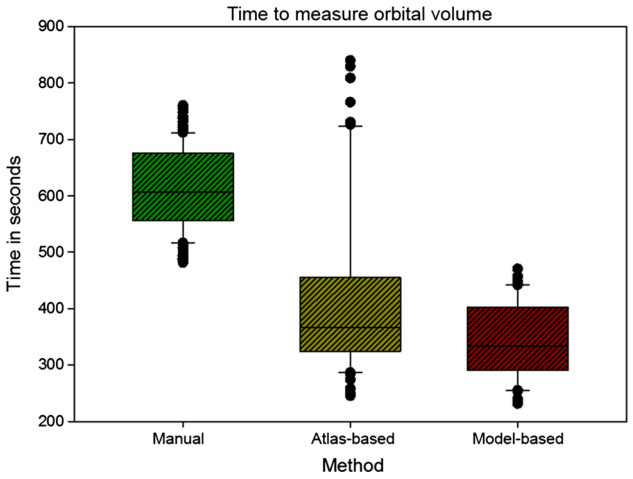

Fig. 7 *Boxplot* of the time it took to measure orbital volume with manual, atlas-based, and model-based segmentation. Each data point represents one measurement. *Error bars* represent one standard deviation from the mean. Manual segmentation took significantly longer time than both atlas-based and model-based segmentation

Discussion

Along with clinical parameters, robust determination of orbital volume is important for assessing patients before and after surgical intervention and for evaluation and treatment of various diseases in and around the orbital cavity. These diseases include trauma [30,31], Graves' disease [32,33], craniosynostosis [34,35], and correction of secondary enophthalmos [36,37]. In most cases, orbital volume is measured to evaluate changes over time (e.g., before and after surgery, to evaluate pathology progression or improvement) or with respect to the contralateral orbit. Available orbital volume measurement methods were evaluated for accuracy and clinical application.

Each segmentation method used to calculate intraorbital volume requires a high-resolution 3-D data. Orbital segmentation has unique challenges (as explained above), mostly due to efforts to decrease radiation exposure during image acquisition and CBCT image characteristics. One such challenge is how segmentation methods handle pseudoforamina.

Reports in the literature describe differences in volume measurements obtained with coronal and axial scans [38]. Atlas- and model-based segmentation methods overcome this discrepancy by determining orbital volume based on 3-D data. Unfortunately, there is no standard way to determine the anterior closing of the orbit. Some authors generate a vertical plane placed at the most anterior point of the lateral orbital wall [39]. However, like us, most authors prefer using the most anterior rim as the anatomical anterior closing [28,29]. This method is independent of the anatomy on the contralateral side, but is more difficult to implement in semi-automatic segmentation modules. In our study, we defined anterior closing using the anterior bony frame of the orbit for all three methods evaluated.

Manual segmentation can be performed with a vast number of segmentation programs and can be used for measuring volume of many different structures, including the orbit. Volume measurements using manual segmentation are very accurate, but are highly dependent upon the evaluator's experience and effort. Additionally, this method is more time-consuming than other, more automated methods, as confirmed by our study results, and it is thus more expensive. Therefore, this method is less commonly used for orbital volume segmentation, and alternative methods have been explored to overcome these disadvantages [40].

Atlas-based segmentation is one of these alternative methods. It is semi-automated and has already been implemented in some clinical software solutions. The amount of user interaction largely depends on the software atlas, the imaging modality, and the 3-D data set image quality. As alternative imaging techniques to CT (e.g., CBCT) become more important and more widely used in the clinical setting, these three factors need to be considered [41,42]. Therefore, we only examined orbital volume calculation methods in CBCT-acquired data sets. Unfortunately, atlas-based segmentation required a considerable amount of manual correction in nearly half of all eyes examined. Anterior closing had to be performed manually in all examined eyes. Although the determination of the anterior orbital rim is fairly distinct, this requirement for manual closing may be the greatest disadvantage of this tool in the actual version. Because manipulations at least to the anterior closing were necessary in all atlas-based segmentations, a comparison without manual correction between atlas- and model-based segmentation seemed to not be meaningful. Nevertheless, if a good data set can be obtained, this technique is fast and accurate and has a relatively low dependence upon user experience. Additionally, atlas-based segmentation is already popular among many

Table 1 Required manual adjustment, usability, and dependence on clinical experience for each segmentation method examined

	Adjustment	Usability	Clinical experience
Manual segmentation	5	2	5
Atlas-based segmentation	3	4	2
Model-based segmentation	3	5	1

Scale: 1–5, where higher numbers mean more desirable

segmentation software users for analysis of the craniomaxillofacial region.

Model-based segmentation is not as well known as manual and atlas-based segmentation. To the best of our knowledge, model-based analyses have not been incorporated into any orbital volume measurement software on the market. However, adaptations have been used with magnetic resonance imaging to segment orbital content [43]. Our results suggest that model-based software can accurately determine orbital volume quickly and in a manner independent of user experience. In fact, the final accuracy was comparable between atlas-based and model-based segmentation. As substantial manual correction was required with atlas-based segmentation to achieve this accuracy, and because only a few corrections were necessary in model-based segmentation, model-based segmentation appears to be suitable for using CBCT images to determine orbital volume. This method also has the major advantage of allowing orbital volume to be calculated with poor-quality (blurred or contains artifacts) image sets. To integrate model-based volume measurements into the clinical setting and computer-assisted surgery, standard software, perhaps based on the analyses used in the current study, needs to be implemented.

Conclusion

For the measurement of orbital volume with cone beam computed tomography, a model-based segmentation technique was utilized and compared with currently used methods. Our results indicate that atlas-based and model-based segmentation are faster and have better usability than manual segmentation. Model-based segmentation of the orbit may be more robust than atlas-based segmentation and is favorable for analyses on poor-quality images. Future studies on model-based orbital volume segmentation will have to evaluate this technique for other image modalities, e.g., MRI.

Acknowledgments The work of MEHW and JTL is funded, in part, by the German Federal Ministry of Education and Research. This work was funded by AOCMF. The sponsor or funding organization had no role in the design or conduct of this research. MB contributed to this work while working at the Institute for Man-Machine Communication, Leibniz University Hannover, Germany.

Conflict of interest No author has any conflict of interest to declare.

References

1. Oppenheimer AJ, Monson LA, Buchman SR (2013) Pediatric orbital fractures. Craniomaxillofac Trauma Reconstr 6(1):9–20. doi:10.1055/s-0032-1332213
2. Fadda MT, Saverio De Ponte F, Bottini DJ, Iannetti G (1996) Study and planning of the surgical procedure for the orbital district in patients affected by craniofacial malformations. J Craniofac Surg 7(3):207–223
3. Gellrich NC, Schramm A, Hammer B, Schmelzeisen R (1999) The value of computer aided planning and intraoperative navigation in orbital reconstruction. Int J Oral Maxillofac Surg 28:52–53
4. Holck DE, Boyd EM Jr, Ng J, Mauffray RO (1999) Benefits of stereolithography in orbital reconstruction. Ophthalmology 106(6):1214–1218. doi:10.1016/S0161-6420(99)90254-3
5. Curley A, Hatcher DC (2010) Cone beam CT-anatomic assessment and legal issues: the new standards of care. Today's FDA 22(4):52–55, 57–59, 61–53
6. Mischkowski RA, Pulsfort R, Ritter L, Neugebauer J, Brochhagen HG, Keeve E, Zoller JE (2007) Geometric accuracy of a newly developed cone-beam device for maxillofacial imaging. Oral Surg Oral Med Oral Pathol Oral Radiol Endod 104(4):551–559. doi:10.1016/j.tripleo.2007.02.021
7. Wang L, Chen KC, Shi F, Liao S, Li G, Gao Y, Shen SG, Yan J, Lee PK, Chow B, Liu NX, Xia JJ, Shen D (2013) Automated segmentation of CBCT image using spiral CT atlases and convex optimization. Medical image computing and computer-assisted intervention. In: MICCAI international conference on medical image computing and computer-assisted intervention, vol 16(Pt 3), pp 251–258
8. Charteris DG, Chan CH, Whitehouse RW, Noble JL (1993) Orbital volume measurement in the management of pure blowout fractures of the orbital floor. Br J Ophthalmol 77(2):100–102
9. Lukats O, Vizkelety T, Markella Z, Maka E, Kiss M, Dobai A, Bujtar P, Szucs A, Barabas J (2012) Measurement of orbital volume after enucleation and orbital implantation. PloS One 7(12):e50333. doi:10.1371/journal.pone.0050333
10. Regensburg NI, Kok PH, Zonneveld FW, Baldeschi L, Saeed P, Wiersinga WM, Mourits MP (2008) A new and validated CT-based method for the calculation of orbital soft tissue volumes. Invest Ophthalmol Vis Sci 49(5):1758–1762. doi:10.1167/iovs.07-1030
11. Metzger MC, Bittermann G, Dannenberg L, Schmelzeisen R, Gellrich NC, Hohlweg-Majert B, Scheifele C (2013) Design and development of a virtual anatomic atlas of the human skull for automatic segmentation in computer-assisted surgery, preoperative planning, and navigation. Int J Comput Assist Radiol Surg 8(5):691–702. doi:10.1007/s11548-013-0818-6
12. Smith DM, Oliker A, Carter CR, Kirov M, McCarthy JG, Cutting CB (2007) A virtual reality atlas of craniofacial anatomy. Plast Reconstr Surg 120(6):1641–1646. doi:10.1097/01.prs.0000282452.22620.25
13. Cohen LD (1991) On active contour models and balloons. CVGIP Image Underst 53(2):211–218
14. McInerney T, Terzopoulos D (1996) Deformable models in medical image analysis: a survey. Med Image Anal 1(2):91–108
15. Cootes T, Hill A, Taylor C, Haslam J (1994) Use of active shape models for locating structures in medical images. Image Vis Comput 12(6):355–365
16. Heimann T, Meinzer HP (2009) Statistical shape models for 3D medical image segmentation: a review. Med Image Anal 13(4):543–563. doi:10.1016/j.media.2009.05.004
17. Lamecker H, Kamer L, Wittmers A, Zachow S, Kaup T, Schramm A, et al (2007) A method for the three-dimensional statistical shape analysis of the bony orbit. In: Freysinger W, Weber S, Caversaccio M (eds) Computer aided surgery around the head: 4th international CAS-H conference proceedings, Pro Business, Berlin, pp 94–97
18. Becker M, Magnenat-Thalmann N (2014) Deformable models in medical image segmentation. Springer, Berlin
19. Deserno TM (2011) Biomedical image processing. Springer Science & Business Media, Berlin
20. Ecabert O, Peters J, Weese J (2006) Modeling shape variability for full heart segmentation in cardiac computed-tomography images.

In: Medical imaging, 2006. International Society for Optics and Photonics, pp 61443R–61443R-61412
21. Zheng Y, Barbu A, Georgescu B, Scheuering M, Comaniciu D (2008) Four-chamber heart modeling and automatic segmentation for 3-D cardiac CT volumes using marginal space learning and steerable features. IEEE Trans Med Imaging 27(11):1668–1681
22. Zhu Z, Li G (2011) Construction of 3D human distal femoral surface models using a 3D statistical deformable model. J Biomech 44(13):2362–2368. doi:10.1016/j.jbiomech.2011.07.006
23. Heimann T, Meinzer HP, Wolf I (2007) A statistical deformable model for the segmentation of liver CT volumes. In: Heimann T, Styner M, van Ginneken B (eds) MICCAI 2007 workshop proceedings: 3D segmentation in the clinic—a grand challenge, pp 161–166
24. Yushkevich PA, Piven J, Hazlett HC, Smith RG, Ho S, Gee JC, Gerig G (2006) User-guided 3D active contour segmentation of anatomical structures: significantly improved efficiency and reliability. NeuroImage 31(3):1116–1128. doi:10.1016/j.neuroimage.2006.01.015
25. Nyström I, Nysjö J, Malmberg F (2011) Visualization and haptics for interactive medical image analysis: Image segmentation in cranio-maxillofacial surgery planning. In: Badioze Zaman H et al (eds) Visual informatics: sustaining research and innovations. IVIC 2011, Part I. LNCS 7066. Springer, Berlin, pp 1–12
26. Becker M, Friese KI, Wolter FE, Gellrich NC, Essig H (2015) Development of a reliable method for orbit segmentation & measuring. In: 2015 IEEE international symposium on medical measurements and applications (MeMeA), accepted May 2015
27. Friese KI, Blanke P, Wolter FE (2011) YaDiV–an open platform for 3D visualization and 3D segmentation of medical data. Vis Comput 27(2):129–139
28. Bite U, Jackson IT, Forbes GS, Gehring DG (1985) Orbital volume measurements in enophthalmos using three-dimensional CT imaging. Plast Reconstr Surg 75(4):502–508
29. Schuknecht B, Carls F, Valavanis A, Sailer HF (1996) CT assessment of orbital volume in late post-traumatic enophthalmos. Neuroradiology 38(5):470–475
30. Ploder O, Klug C, Voracek M, Burggasser G, Czerny C (2002) Evaluation of computer-based area and volume measurement from coronal computed tomography scans in isolated blowout fractures of the orbital floor. J Oral Maxillofac Surg 60(11):1267–1272 discussion 1273–1264
31. Scolozzi P, Jaques B (2008) Computer-aided volume measurement of posttraumatic orbits reconstructed with AO titanium mesh plates: accuracy and reliability. Ophthalmic Plast Reconstr Surg 24(5):383–389. doi:10.1097/IOP.0b013e318185a72c
32. Lutzemberger L, Salvetti O (1998) Volumetric analysis of CT orbital images. Med Biol Eng Comput 36(6):661–666
33. Comerci M, Elefante A, Strianese D, Senese R, Bonavolonta P, Alfano B, Bonavolonta B, Brunetti A (2013) Semiautomatic regional segmentation to measure orbital fat volumes in thyroid-associated ophthalmopathy. A validation study. Neuroradiol J 26(4):373–379
34. Bentley RP, Sgouros S, Natarajan K, Dover MS, Hockley AD (2002) Changes in orbital volume during childhood in cases of craniosynostosis. J Neurosurg 96(4):747–754. doi:10.3171/jns.2002.96.4.0747
35. Festa F, Pagnoni M, Valerio R, Rodolfino D, Saccucci M, d'Attilio M, Caputi S, Iannetti G (2012) Orbital volume and surface after Le Fort III advancement in syndromic craniosynostosis. J Craniofac Surg 23(3):789–792. doi:10.1097/SCS.0b013e31824dbeec
36. Fan X, Li J, Zhu J, Li H, Zhang D (2003) Computer-assisted orbital volume measurement in the surgical correction of late enophthalmos caused by blowout fractures. Ophthalmic Plast Reconstr Surg 19(3):207–211
37. Manson PN, Grivas A, Rosenbaum A, Vannier M, Zinreich J, Iliff N (1986) Studies on enophthalmos: II. The measurement of orbital injuries and their treatment by quantitative computed tomography. Plastic Reconstr Surg 77(2):203–214
38. Kwon J, Barrera JE, Most SP (2010) Comparative computation of orbital volume from axial and coronal CT using three-dimensional image analysis. Ophthalmic Plastic Reconstr Surg 26(1):26–29. doi:10.1097/IOP.0b013e3181b80c6a
39. Whitehouse RW, Batterbury M, Jackson A, Noble JL (1994) Prediction of enophthalmos by computed tomography after 'blow out' orbital fracture. Br J Ophthalmol 78(8):618–620
40. Schramm H, Ecabert O, Peters J, Philomin V, Weese J (2006) Towards fully automatic object detection and segmentation. In: Medical imaging, 2006. International Society for Optics and Photonics, pp 614402–614402-614410
41. Zizelmann C, Gellrich NC, Metzger MC, Schoen R, Schmelzeisen R, Schramm A (2007) Computer-assisted reconstruction of orbital floor based on cone beam tomography. Br J Oral Maxillofac Surg 45(1):79–80. doi:10.1016/j.bjoms.2005.06.031
42. Kolk A, Pautke C, Schott V, Ventrella E, Wiener E, Ploder O, Horch HH, Neff A (2007) Secondary post-traumatic enophthalmos: high-resolution magnetic resonance imaging compared with multislice computed tomography in postoperative orbital volume measurement. J Oral Maxillofac Surg 65(10):1926–1934. doi:10.1016/j.joms.2006.06.269
43. Li Z, Chui CK, Cai Y, Amrith S, Goh PS, Anderson JH, Teo J, Liu C, Kusuma I, Siow YS, Nowinski WL (2002) Modeling of the Human Orbit from MR Images. In: Paper presented at the anonymous medical image computing and computer-assisted intervention—MICCAI, Tokyo, Japan, Sep 25–28